Available online at www.sciencedirect.com

SciVerse ScienceDirect

Ceramics International 39 (2013) 4627–4631

CERAMICS INTERNATIONAL

www.elsevier.com/locate/ceramint

Short communication

Ablative property of laminated ZrB_2–SiC ceramics under oxyacetylene torch

Fengjuan Zuo, Laifei Cheng*, Liuyi Xiang, Litong Zhang, Liangjun Li

Key Laboratory of Science and Technology on Thermostructural Composite Materials, Northwestern Polytechnical University, Xi'an 710072, People's Republic of China

Received 8 August 2012; received in revised form 7 October 2012; accepted 8 October 2012
Available online 23 October 2012

Abstract

Two kinds of laminated ZrB_2–SiC ceramics were successfully fabricated by aqueous tape casting, laminating and hot-pressing. The first one was alternately composed of ZrB_2+36 vol% SiC layers and ZrB_2+20 vol% SiC layers with sintering aid of 5 vol% B_4C. The second one was achieved by inserting an aquadag interlayer between two different ZrB_2–SiC layers. The ablation experiments were carried out on an oxyacetylene torch flame with a temperature of about 3000 °C. Both ceramics exhibited zero ablation in the macroscopic level after ablation for 20 s, showing outstanding ablation resistance. However, ablation oxidation layer of the second ceramic was thinner than that of the first one microscopically, which was mainly attributed to full densification of the surface ablation layer. The aquadag layer promoted sintering of laminated ZrB_2–SiC ceramics at elevated temperatures.

Keywords: Laminated ZrB_2–SiC ceramics; Oxyacetylene torch flame; Ablation resistance

1. Introduction

Ultra-high temperature ceramics (UHTCs) have paid more and more attention in recent years because of their unique and excellent combination of high melting points, good thermal shock resistance and good ablation/oxidation resistance. They have been considered as the promising candidates for high temperature structural applications, including thermal protection systems, atmospheric re-entry, rocket propulsion systems, leading edge, nose cone and scramjet engine components for hypersonic flight vehicles, etc [1–3].

Zirconium diboride (ZrB_2) occupies a dominant position in the family of UHTCs due to its remarkable physico-chemical properties, which makes it be an attractive material [4–6]. However, it is scarcely used alone due to its poor oxidation resistance. Several studies have demonstrated that the addition of SiC increased oxidation resistance and mechanical properties of the ZrB_2 ceramics by improving its densification [7–12]. Laminated structures can be found everywhere in nature, such as biological hard tissues, shells and teeth. Laminated ceramics are more designable, including microstructure and properties. Through proper design, toughness and thermal shock resistance of laminated ceramics can be superior to those of the individual constituents [13,14]. Two main methods can be used to improve the performance of laminated ceramics over monolithic ceramics. One is the introduction of weak interfaces [15,16], such as boron nitride (BN) and graphite. The other is making the presence of residual stresses [17,18]. Cracks deflect at and move along the weak interface [19]. The residual stresses in laminated ceramics result from the mismatch in elastic modulus, shrinkage and coefficient of thermal expansion (CTE) among different layers, and can be tailored for optimizing resistance of the crack growth.

In recent years, many researchers have been focused on the mechanical properties of laminated ZrB_2–SiC ceramics [20–22]. However, ablation behaviors of laminated ZrB_2–SiC ceramics have been rarely investigated. In this paper, laminated ZrB_2–SiC ceramics were prepared by aqueous tape casting, laminating and hot-pressing. The central goal of the

*Corresponding author. Tel.: +86 29 88494616; fax: +86 29 88494620.
E-mail addresses: chenglaifei@163.com, chenglf@nwpu.edu.com (L. Cheng).

0272-8842/$ - see front matter © 2012 Elsevier Ltd and Techna Group S.r.l. All rights reserved.
http://dx.doi.org/10.1016/j.ceramint.2012.10.179

Table 1
Powders used for laminated ZrB_2–SiC ceramics sample preparation.

Powders	Source	Particle Size (μm)	Purity (%)
ZrB_2	Northwest Institute for Non-ferrous Metal Research, China	1.1	99.5
SiC	Weifang Kaihua Micro-powder Co.,Ltd.,China	0.5	99.5
B_4C	Weifang Kaihua Micro-powder Co.,Ltd.,China	1	99
Aquadag	Shanghai St-nano Science and Technology Co.,Ltd.,China	1	99

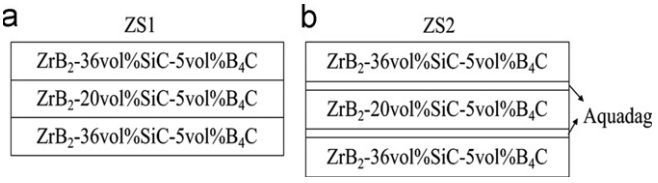

Fig. 1. Schematic illustration of two kinds of laminated structure.

present study is to investigate the ablation behavior of the laminated ZrB_2–SiC ceramics and to discuss the ablation mechanism.

2. Experimental

2.1. Preparation of laminated ZrB_2–SiC ceramics

Commercially available raw powders used for preparation of the laminated ZrB_2–SiC ceramics are listed in Table 1. The laminated architecture was decided according to the differences in the thermal expansion coefficients of two adjacent components, which can lead to a strain mismatch during cooling from the sintering temperature [23]. In this paper, two kinds of laminated ZrB_2–SiC ceramics were symmetric in macrostructure. Fig. 1 illustrated the schematic macrostructure for the laminated ZrB_2–SiC ceramics. The first one, named as ZS1, was alternately composed of ZrB_2+36 vol% SiC layers and ZrB_2+20 vol% SiC layers, and the second one, named as ZS2, was alternately composed of ZrB_2+36 vol% SiC layers, aquadag layers and ZrB_2+20 vol% SiC layers. Aquadag is a water-based colloidal graphite suspension. Both laminated ZrB_2–SiC ceramics had the external layer of ZrB_2+36 vol% SiC layer. The sintering aid for the ZrB_2–SiC layers was 5 vol% B_4C. The thickness of the ZrB_2–SiC layers in ZS1 was the same (Fig. 1a). The aquadag was brushed between the ZrB_2–SiC layers, which was much thinner than the ZrB_2–SiC layers (Fig. 1b).

The ZrB_2–SiC layers were produced by tape casting technique. Aqueous ZrB_2–SiC slurries were prepared by mixing the powders and dispersing the mixture into distilled water in a certain proportion. Slurries were milled with zirconium balls for 24 h. After adding a binder and a plasticizer, the slurries were milled for 12 h. The slurries were homogenized by degassing under vacuum for removal of air bubbles. Tape casting was performed on the self-made cast mold with a gap height of 800 μm which control layer thickness. It can be adjusted by the height of a glass plate embedded in the mold. After drying freely in open air at ambient temperature for 7–8 h, the green tapes were stacked in sequence until the desired compositions were obtained. The laminated bodies were pressed at room temperature by cold isostatic pressing. After removing binder at 500 °C for 1 h in a graphite die lined with a BN-sprayed graphitized foil, the bodies were sintered at 1950 °C for 1 h under a uniaxial pressure of 30 MPa in argon atmosphere.

2.2. Ablation tests and microstructure analysis

The density of the as-sintered specimens was measured by the Archimedes' immersion method according to ASTM C-20standard. Ablation tests were carried out in an oxyacetylene torch environment. During the test, the specimens (diameter: 30 mm; height: 10 mm) were mounted in a water-cooled concave steel holder and vertically exposed to the flame for 20 s. The distance between the nozzle tip of the oxyacetylene gun and the specimen surface was 10 mm and the inner diameter of the tip was 2.5 mm. The weight change (before and after the test) was assessed from the specimen dimension change as measured by a vernier caliper with an accuracy of 0.002 mm and the ablation rate of each specimen was calculated. The heat flux and the temperature in the center of the specimen were reported to be respectively about 4186 kW/m^2 ($\pm$10% error) and 3000 °C [24].

The microstructure and the phase composition of the laminated ZrB_2–SiC ceramics before and after ablation were analyzed with a scanning electron microscope (SEM, S-4700, Hitachi, Japan) and an X-ray diffractometer (XRD, D8ADVANCE, Bruker, Germany).

3. Results and discussion

The relative bulk density of the as-sintered ZS1 and ZS2 was 99.4% and 99.7%, respectively. The high density was owed to the sintering temperature and sintering additives. Fig. 2(a) and (b) show the cross-section morphology of ZS1 and ZS2 before ablation under oxyacetylene torch flame, and Fig. 2(c) and (d) show the interfacial morphology of ZS1 and ZS2. From Fig. 2(a) and (b), no open or closed pores as well as interfacial cracks are observed. Fig. 2 was marked 1, 2 and 3, which respectively means ZrB_2+36 vol%SiC layer, ZrB_2+20 vol% SiC layer and aquadag layer. As we can see, the thickness of the ZrB_2+36 vol% SiC layers is about 100 μm and that of the ZrB_2+20 vol% SiC layers is about 60 μm (Fig. 2(a)).

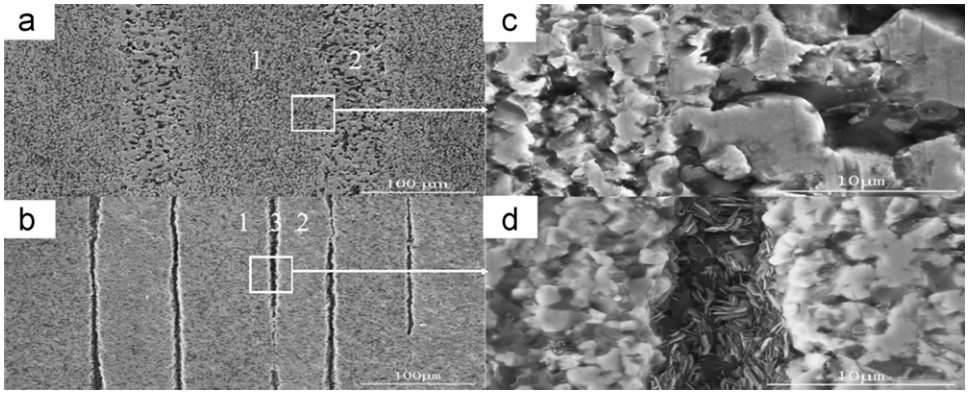

Fig. 2. SEM micrographs of the cross-sectional of ZS1 and ZS2 before ablation.

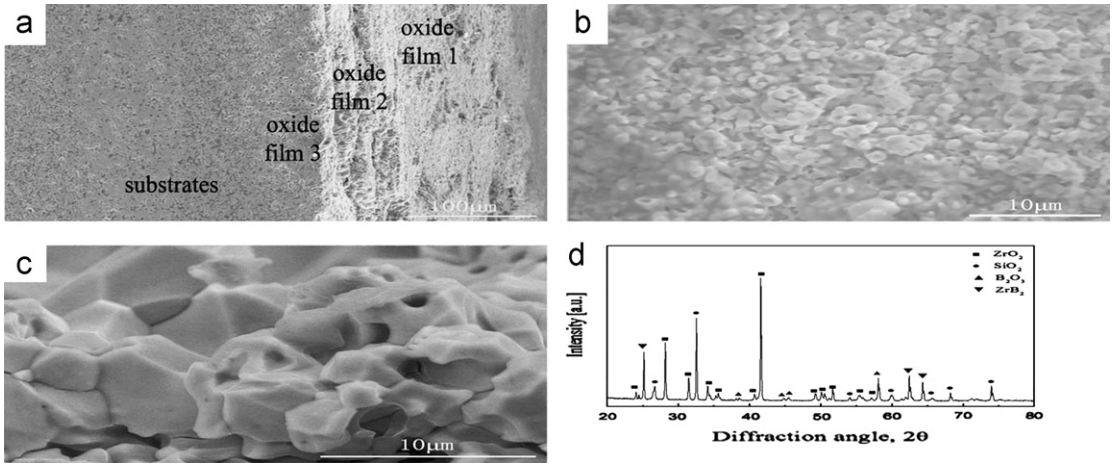

Fig. 3. SEM and XRD of ZS1 samples after ablation for 20 s.

The interfaces and interface-layers of the laminated ZrB_2–SiC ceramics are clear and almost straight, as shown in Fig. 2(a) and (b). The ZrB_2 particulate in ZrB_2+36 vol% SiC layer is smaller than in ZrB_2+20 vol% SiC, due to the different content of SiC (Fig. 2(c)). The SiC particulate was homogenously distributed in the ZrB_2 particulate and no agglomeration was detected. The aquadag layer is in interlaced distribution (Fig. 2(d)). In addition, the ZrB_2–SiC layers of ZS2 are obviously denser than those of ZS1.

Fig. 3 shows the morphology of as-produced ZS1 after ablation for 20 s. The thickness of ablation oxidation layer is about 150 μm (Fig. 3(a)). Fig. 3(a) shows that the first oxide film is dense and smooth whereas the second oxide film is rugged with many micro-cracks and voids. The bonding strength at the interface between the second oxide film and the third oxide film is weakest among all layers due to the coefficient of the thermal expansion mismatch between the ZrO_2 and unaltered ZrB_2. There are many small voids in the third oxide film, but the bonding between this film and substrates is good. Fig. 3(b) and (c) show the surface morphology of oxide scale with different magnification. It can be seen that there appeared still a large number of holes and many bubbles on the surface (Fig. 3(b)). The holes were produced by burst of bubbles (Fig. 3(c)). The formation of bubbles means that the diffusion of the formed gaseous products through the oxidation layer was slower than that of O_2.

The morphologies of as-produced ZS2 after ablation for 20 s are shown in Fig. 4. The thickness of ablation oxidation layer on ZS2 is about 90 μm (Fig. 4(a)), which is smaller than that on ZS1. The surface morphology of ZS1 and ZS2 is similar, but ZS2 had smaller denuded holes than ZS1. Fig. 4(a) and Fig. 3(a) show that the oxide film of ZS2 is denser and has a better interfacial bonding with the substrates than that of ZS1. From Fig. 4(b) and (c), it can be found that the oxide film has been molten under the ablation condition. The oxide grains of ZS2 are finer than those of ZS1. It can be concluded that ZS2 has a better ablation resistance than ZS1. As a weak interlayer, the aquadag layer possesses low modulus and high thermal conductivity. In the hot-pressing process, it can decrease the pressure gradient in ZS2 and promote the rearrangement of the particles. As a result, ZS2 was sintered more easily and denser than ZS1.

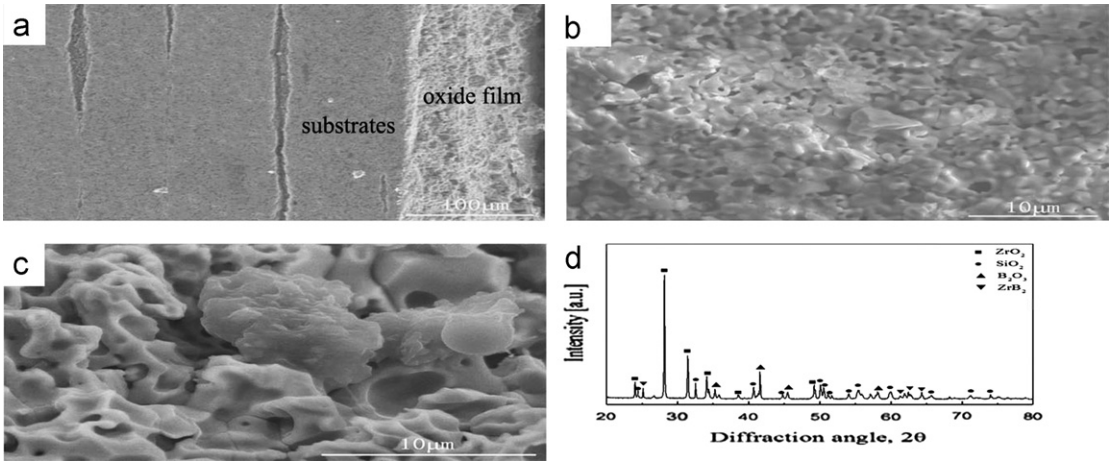

Fig. 4. SEM and XRD of ZS2 samples after ablation for 20 s.

From XRD analysis of the ablation surface, it can be indicated that the oxidation products were ZrO_2 (white phase), SiO_2 and B_2O_3 (Fig. 3(d), Fig. 4(d)). The main expected reactions during the ablation process are as follows

$$ZrB_2\ (s)+5/2\ O_2\ (g)\rightarrow ZrO_2(s)+B_2O_3\ (l) \quad (1)$$

$$B_2O_3\ (l)\rightarrow B_2O_3\ (g) \quad (2)$$

$$SiC\ (s)\rightarrow SiC\ (l) \quad (3)$$

$$SiC\ (l)+2/3\ O_2\ (g)\rightarrow SiO_2\ (l)+CO\ (g) \quad (4)$$

$$SiC\ (l)+O_2\ (g)\rightarrow SiO\ (g)+CO\ (g) \quad (5)$$

$$SiO2\ (l)\ \rightarrow SiO_2\ (g) \quad (6)$$

$$SiO2\ (l)\rightarrow SiO\ (g)+1/2\ O_2\ (g) \quad (7)$$

In fact, both SiO_2 and B_2O_3 had high vapor pressures, so they vaporized quickly in ablation (reactions (2) and (6)). During ablation, active oxidation of SiC takes place (reactions (4), (5) and (7)), and SiC has no crucial role for improvement of the ablation resistance longer. However, the volatilization of ZrO_2 was negligible since its vapor pressure was lower than SiO_2. Under the ablation condition, the ZrO_2 film was not blown off by oxyacetylene torch flame, protecting the surface from further ablation. As implied by the above analysis, the aquadag layer and ZrO_2 film appear to protect the laminated ceramic from catastrophic ablation.

4. Conclusions

Two laminated ZrB_2–SiC ceramics were prepared by aqueous tape casting, laminating and hot-pressing. ZS1 was alternately composed of ZrB_2+36 vol% SiC layers and ZrB_2+20 vol% SiC layers with sintering aid of 5 vol% B_4C. ZS2 was obtained by brushing an aquadag interlayer between two different ZrB_2–SiC layers. The ablation behaviors of the laminated ZrB_2–SiC ceramics were investigated by oxyacetylene torch. The main surface ablation product of laminated ZrB_2–SiC ceramics was ZrO_2. No micro-cracks or spallation was observed after ablation. The results indicated that the laminated ZrB_2–SiC ceramics exhibited an excellent thermal shock resistance. However, ZS2 performed a better ablation resistance than ZS1, which was owed to the existence of the aquadag interlayer. In conclusion, laminated ZrB_2–SiC ceramics exhibited excellent ablation resistance close to 3000 °C for 20 s in oxidizing environment and a dense oxide film was formed after ablation, which suggested they were potential candidates for the leading edges.

References

[1] W.G. Fahrenholtz, G.E. Hilmas, I.G. Talmy, J.A. Zaykoski, Refractory diborides of zirconium and hafnium, Journal of the American Ceramic Society 90 (2007) 1347–1364.
[2] S.R. Levine, E.J. Opila, M.C. Halbig, J.D. Kiser, M. Singh, J.A. Salem, Evaluation of ultra high temperature ceramics for aeropropulsion use, Journal of the European Ceramic Society 22 (2002) 2757–2767.
[3] D.M. Van Wie, D.G. Drewry, D.E. King, C.M. Hudson, The hypersonic environment: required operating conditions and design challenges, Journal of Materials Science 9 (2004) 5915–5924.
[4] A.L. Chamberlain, W.G. Fahrenholtz, G.E. Hilmas, D.T. Ellerby, High-strength zirconium diboride-based ceramics, Journal of Ceramic Society 87 (2004) 1170–1172.
[5] F. Monteverde, Beneficial effects of an ultra-fine a-SiC incorporation on the sinterability and mechanical properties of ZrB_2, Applied Physics A 82 (2006) 329–337.
[6] K. Upadhya, J.M. Yang, W.P. Hoffman, Materials for ultrahigh temperature structural applications, Journal of the American Ceramic Society Bulletin 76 (1997) 51–56.
[7] S. Zhu, W.G. Fahrenholtz, G.E. Hilmas, S. Zhu, Influence of silicon carbide particle size on the microstructure and mechanical properties of zirconium diboride–silicon carbide ceramics, Journal of the European Ceramic Society 27 (2007) 2077–2083.
[8] S.S. Huang, A.L. Vailiev, N.P. Padture, Improved processing and oxidation-resistance of ZrB_2 ultra-high temperature ceramics containing SiC nanodispersoids, Material Science Engineering A 464 (2007) 216–222.
[9] F. Monteverde, A. Bellosi, Oxidation of ZrB_2-based ceramics in dry air, Journal of the Chemical Society 150 (2003) 552–559.

[10] Y. Yan, Z. Huang, S. Dong, D. Jiang, Pressureless sintering of high-density ZrB_2–SiC ceramic composites, Journal of the Ceramic Society 88 (2006) 3589–3592.
[11] M.M. Opeka, I.G. Talmy, E.J. Wuchina, J.A. Zaykoski, S.J. Causey, Mechanical, thermal, and oxidation properties of refractory hafnium and zirconium compound, Journal of the European Ceramic Society 19 (1999) 2405–2414.
[12] S.N. Karlsdottir, J.W. Halloran, Oxidation of ZrB_2–SiC: influence of SiC content on solid and liquid oxide phase formation, Journal of the American Ceramic Society 92 (2009) 481–486.
[13] S. Bueno, C. Baudlń, Layered materials with high strength and flaw tolerance based on alumina and aluminium titanate, Journal of the European Ceramic Society 27 (2007) 1455–1462.
[14] G. de Portu, L. Micele, G. Pezzotti, Lamiated ceramic structures from oxide systems, Composites Part B Engineering 37 (2006) 556–567.
[15] Y.Y. Gao, S.Y. Zheng, K.C. Zhu, Analysis of mechanical properties and SEM for laminated SiC/W composites, Materials Science 50 (2001) 358–363.
[16] C.A. Wang, Y. Huang, Q.F. Zan, H. Guo, S.Y. Cai, Biomimetic structure design-a possible approach to change the brittleness of ceramics in nature, Materials Science Engineering C 11 (2000) 9–12.
[17] V.M. Sglavo, M. Bertoldi, Design and production of ceramic laminates with high mechanical reliability, Composites Part B Engineering 37 (2006) 481–489.
[18] M. Lugovy, V. Slyunyayev, N. Orlovskaya, G. Blugan, J. Kuebler, M. Lewis, Apparent fracture toughness of Si_3N_4-based laminates with residual compressive or tensile stresses in surface layers, Acta Materialia 53 (2005) 289–296.
[19] M. Pavese, P. Fino, A. Ortona, C. Badini, Potential of SiC multilayer ceramics for high temperature application in oxidising environment, Ceramics International 34 (2008) 197–203.
[20] A.J. Blattner, R. Lakshminarayanan, D.K. Shetty, Toughening of layered ceramic composites with residual surface compression:effects of layer thickness, Engineering Fracture Mechanics 68 (2001) 1–7.
[21] P. Zhou, P. Hu, X.H. Zhang, W.B. Han, Laminated ZrB_2–SiC ceramic with improved strength and toughness, Scripta Materialia 64 (2011) 276–279.
[22] Z.H. Lü, D.L. Jiang, J.X. Zhang, Q.L. Lin, Processing and properties of ZrB_2–SiC composites obtained by aqueous tape casting and hot pressing, Ceramics International 37 (2011) 293–301.
[23] S. Ho, C. Hillman, F.F. Lange, Z. Suo, Surface cracking in layers under biaxial residual compressive stress, Journal of the American Ceramic Society 78 (1995) 2353–2359.
[24] K. Upadhya, J.M. Yang, W.P. Hoffman, Materials for ultra-high temperature structural applications, Journal of the American Ceramic Society Bulletin 12 (1997) 51–56.